Analytical Model of Current-Force Characteristics of a Combined Radial-Axial Magnetic Bearing

Philipp Imoberdorf[1,a], Thomas Nussbaumer[2,b], Johann W. Kolar[1,c]
[1]Power Electronic Systems Laboratory, ETH Zurich, 8092 Zurich, Switzerland
[2]Levitronix GmbH Technoparkstrasse 1, 8005 Zurich, Switzerland
[a]imoberdorf@lem.ee.ethz.ch, [b]nussbaumer@levitronix.com, [c]kolar@lem.ee.ethz.ch

Abstract: In today's industry high-speed and high-power-density drives are attracting much interest, e.g. for applications with mesoscale gas turbine generator systems or turbocompressors for fuel cells. In all high-speed drive systems the bearing technology is a key component. Therefore, this paper presents the analysis of an active magnetic bearing suitable for a permanent magnet machine, being part of a high-speed electrical drive system. The analysis has its focus on the detailed characterization of the magnetic forces, the coupling between the different axes and the verification of the theoretical considerations by means of 3D-FEM simulations. To understand the behavior of the bearing forces is needed to implement the position control to the prototype of the bearing system, which already has been built.

Keywords: Magnetic Bearing, Coupling Effects, Permanent Magnet Machine, Stability

Introduction

In the industry the demand for high-speed and high-power-density drives was increasing over the last few years, and the trend to more compact and higher speed drives still continues [1]. An example is the PCB drilling industry, where the trend is to produce smaller diameter holes. In order to attain the same productivity as today the drilling machines have to rotate at much higher speeds (more than 300,000 rpm). The trend for turbocompressors is towards smaller power ratings and with the scaling of turbo machinery, they therefore require higher operating speeds [2], [3]. One application is in a fuel cell air compressor that requires 120,000 rpm at 12 kW [4] and another is in a 70,000 rpm, 131 kW turbo compressor connected to a PM machine and inverter [5]. Future automotive fuel cells will require low power air compressors, which are small and lightweight, and directly driven by high-speed electrical drives. Ultra-micro gas turbines with power outputs up to several hundred watts are being investigated for use in portable power applications [6].

High rotational speeds however, pose some big challenges to the bearing system. Therefore, this paper presents the design and analysis of an active magnetic bearing suitable for a permanent magnet machine, which is part of a high-speed electrical drive system. The machine and the magnetic bearings are integrated into one system and the power and control electronics for both drive and bearing are optimized for high-speed operation and minimal volume. The motivation for this work is to achieve a compact design of a combined radial axial magnetic bearing to ensure a compact drive system.

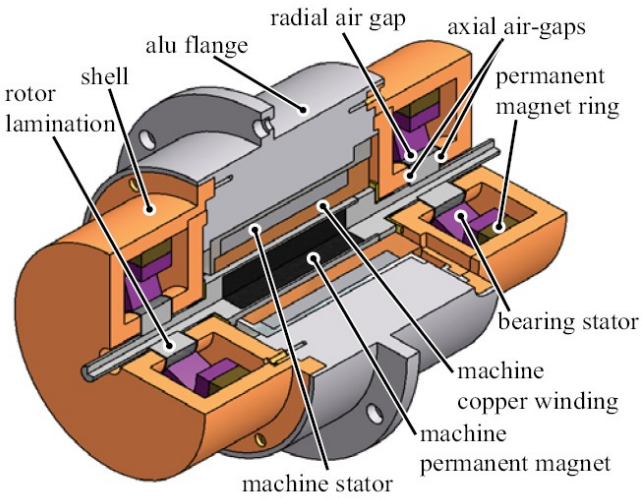

Fig. 1. Cut-away view of the electrical drive and the two radial-axial bearing units mounted on two sides.

Concept / System

The active magnetic bearing is constructed together with a 1 kW, 500'000 rpm permanent-magnet machine developed at ETH Zurich [1]. The machine and the magnetic bearings are integrated into one system and the power and control electronics for both the drive and bearing are optimized for high-speed operation and minimal volume. The rotor is driven by a 1 kW permanent magnet synchronous machine and a bearing unit is placed at each end of the rotor as depicted in Fig. 1. The overall size of the system is a maximum diameter of 55 mm and a rotor length of 96 mm. Most of the active magnetic bearing systems have two separate bearings for the axial and the radial direction. This is the easiest way to produce a magnetic bearing but it also requires more space for the two separate devices. In order to reduce the overall size of the bearing and drive system, which is an important consideration in ultra-compact high-speed machines, the combination of the radial and axial bearing is one attractive possibility. The chosen concept, depicted in Fig. 2, combines the two bearings by using a radially magnetized permanent magnet ring as source of the bias flux for both the radial and the axial bearing [7]. The bias flux created by the permanent magnet ring alone does not provide any force. It has to be superimposed by a control flux for both the radial and the axial bearing force. In Fig. 2, both the radial and the axial control flux paths are depicted. In one air gap, the bias flux and the control flux add together, whereas in the opposing air gap they subtract. The resulting difference of magnetic flux density in these two air gaps creates the carrying force and can be controlled by the sign and amplitude of the control current in the control coils. The bearing force in one air-gap is deduced from the stored magnetic energy in the air-gap. Applying this to the case, where there are two opposite forces and the magnetic field is created by a bias flux density B_0 combined with a control flux density B_c results in a total magnetic force acting on the rotor according to

$$F = \frac{2A_\delta}{\mu_0} \cdot B_0 B_c \,, \tag{1}$$

where A_δ is the active pole shoe area. For small deflections x of the shaft position the bearing force F_x in x-direction can be linearised for very simple cases as

$$F_x = k_{ix} \cdot i_x + k_{rx} \cdot x \,, \tag{2}$$

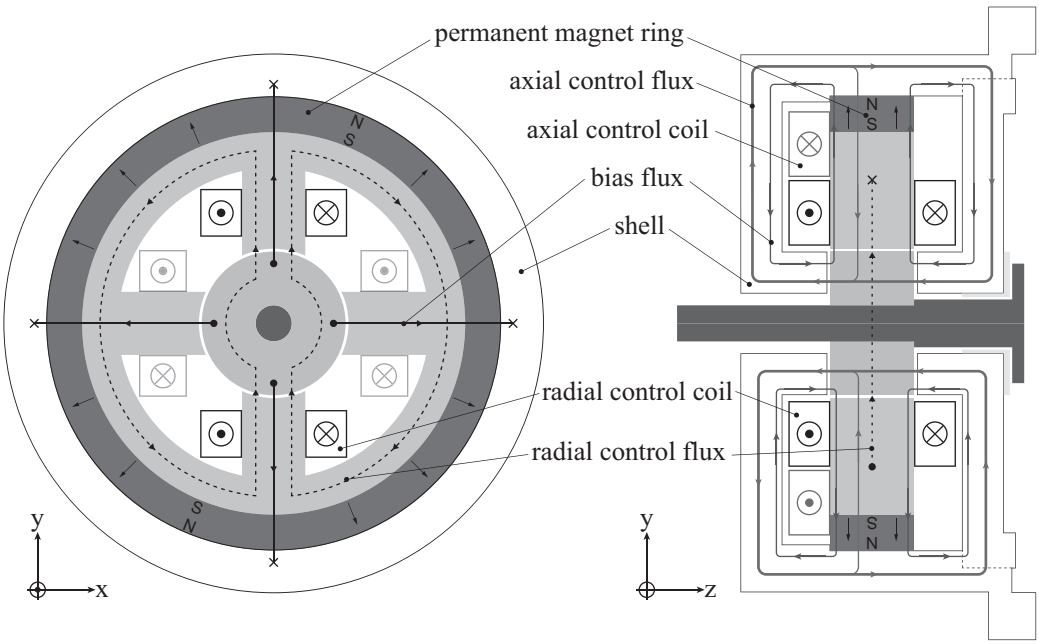

Fig. 2. Axial and radial cut view showing the magnetic flux paths.

where k_{ix} is the force-current factor and k_{rx} the force-displacement factor in x-direction. k_r is also called negative stiffness of the magnetic bearing since without a control current the force acts as a negative spring force and thus is instable. The idea is to characterize the magnetic bearing via these two parameters. For the shown concept it will be shown that the relation is not that simple.

Analysis and Modeling of the Bearing Forces

Equivalent Circuit Model. In order to characterize the bearing and to analyze the system stability for different points of operation a model of the combined radial-axial magnetic bearing has to be built. In a first approach, the magnetic bearing is modeled as an equivalent magnetic circuit as depicted in Fig. 4. Hereby, the permanent magnet is modeled by a magnetic voltage source θ_{PM} in series with the reluctance R_{PM}. The reluctances of the airgaps are dependent on the dimensions of the airgap and are defined as

$$R_\delta = \frac{l_\delta}{\mu_0 A_\delta}, \tag{3}$$

for a homogenous field distribution within the gap. In reality, also stray flux effects have to be considered by adding reluctances for the stray paths as well. Performing comparative 3D-FEM simulations help to identify the relevant stray paths. For this reason a simplified model of the axial part of the bearing, as shown in Fig. 3(a), was modeled and the paths of the magnetic flux were analyzed. Including the most relevant stray flux paths in an equivalent circuit as seen again in Fig. 3(a) as an overlay, allowed comparing the results of the equivalent circuit with the FEM simulation results. In Fig. 4, the equivalent model of the complete combined radial-axial magnetic bearing, the stray reluctances are were incorporated in the main reluctances for the sake of simplicity.

The currents injected in the control coils of the magnetic bearing are modeled as magnetic voltage sources θ_{cx+}, θ_{cx-}, θ_{cy+}, θ_{cy-} and θ_{cz-}. As the control coils for each radial bearing are connected in series, the two corresponding voltage sources are oriented such that their magnetic fluxes add together in the main magnetic path. In Fig. 4 the main magnetic paths for the three bearing directions are illustrated by the bold gray lines. Due to the equal ampere-turns in each axis, the condition

$$\theta_{cx+} = \theta_{cx-} = \theta_{cx} \text{ and } \theta_{cy+} = \theta_{cy-} = \theta_{cy}, \tag{4}$$

is true. Assuming the rotor in its center position, the radial airgap reluctances R_{x+}, R_{x-}, R_{y+} and R_{y-} are equal. Therefore, the magnetic flux created by θ_{cx+} and θ_{cx-} will flow entirely in the main magnetic path depicted in bold gray on the left side of Fig. 4. However, if we assume the rotor to be displaced in x-direction, the reluctances R_{x+} and R_{x-} differ and therefore not the entire flux will flow

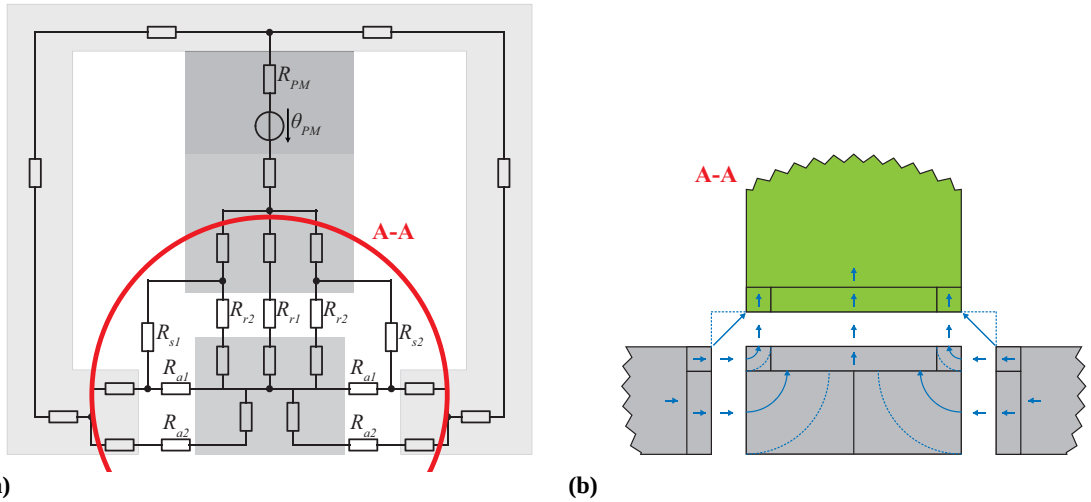

Fig. 3. (a) Equivalent circuit of axial bearing fluxes and (b) details of fluxpaths as observed in 3D-FEM simulation.

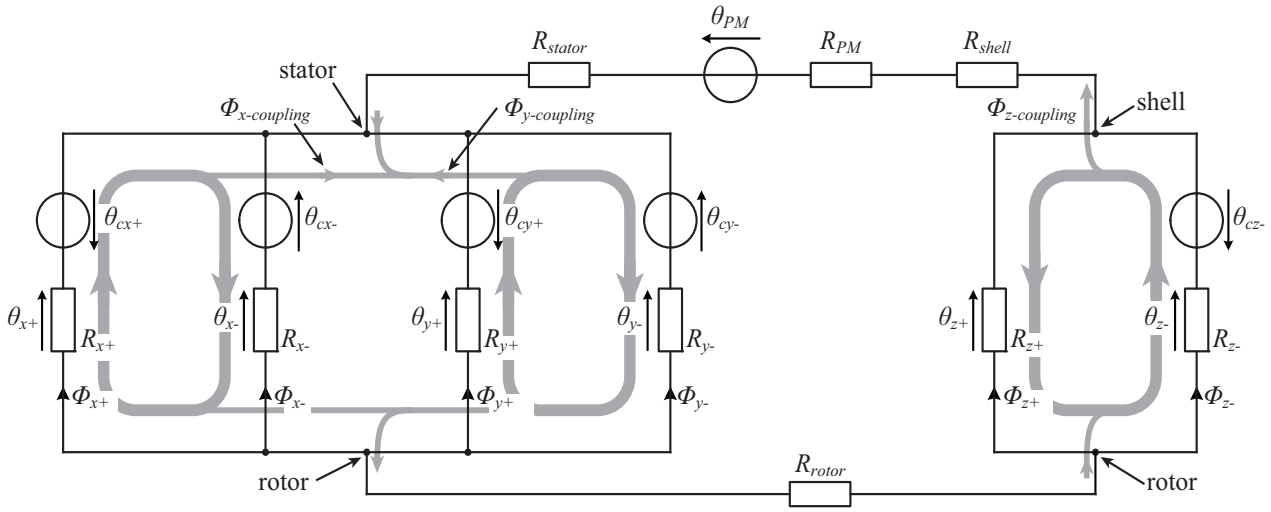

Fig. 4. Equivalent magnetic circuit for the magnet fluxes of the combined radial-axial bearing.

in the main path. Part of it will flow through the airgaps in the *y*-axis and the *z*-axis and consequently constitute a coupling flux $\Phi_{x\text{-}coupling}$. Thus, if all the radial reluctances are equal – the rotor is then in its center position – the *y*-axis is independent of the control flux created by the magnetomotive force θ_{cx}. On the other hand if the rotor is deflected from its center position the four radial airgap reluctances are not equal anymore. Due to such an asymmetry the magnetomotive force θ_{cx} can also create a force in the *y*-direction. The same reasoning can be done for the flux created by θ_{cz}. Since the permanent magnet ring has a big cross section, its reluctance is of comparable dimension as the airgap reluctances and therefore the permanent magnet reluctance is not a perfect separation of the axial and the radial magnetic flux paths. Therefore, part of the flux created by θ_{cz} will flow as a coupling flux $\Phi_{z\text{-}coupling}$ though the radial airgaps.

Verification with 3D-FEM. As the nonlinear relations between the magnetic forces and the operating point parameters are used in the control for the bearing, the validity of the simplified analytical model has to be verified. This has been done by modeling the magnetic bearing in a 3D-FEM simulation software [8]. In all the simulations both the radial and the axial airgaps are set to 500 µm. The results of the simulations showed that the magnetic flux is not entirely confined in the airgap area but also takes some stray paths. This fact has to be considered in the analytical model of the equivalent magnetic circuit. This was done by adding stray path reluctances where the dimensions could be deduced from the FEM simulations.
For the comparison in Fig. 5 the relation of the axial force and the axial control flux was studied. In

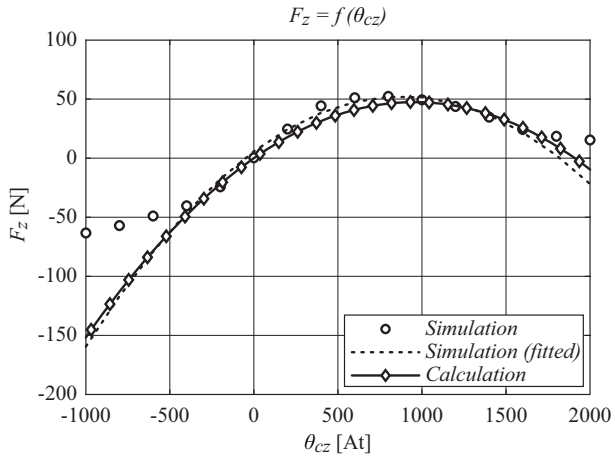

Fig. 5. Comparison of the axial force-current relation derived by calculation and by a 3D-FEM simulation.

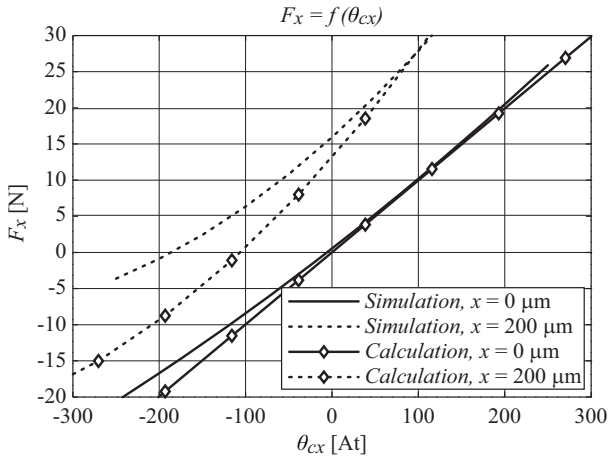

Fig. 6. Comparison of the radial force-current relation for two different radial positions derived by calculation and by a 3D-FEM simulation.

the simulation the stator material is defined as a real magnetic iron. Therefore, saturation effects occur for high magnitudes of current injection into the control coils. The outermost dots on each side in Fig. 5 were ignored for the fitted curve of the simulation results because saturation effects in the range of high control fluxes are not considered in the analytical model. As can be seen in the chart, the force calculated with the equivalent magnetic circuit coincides well with the results from the 3D-FEM simulation, which confirms the proposed model. In Fig. 6 the effect of a deflected rotor on the radial force is depicted. In one case the rotor is in its center position and no other current than i_x is present. The second pair of curves shows the situation when the rotor is deflected in the positive x-direction by 200 µm. Again, an acceptable match of the simulation and calculation results can be observed. This proves the presented analytical model which therefore can be used for the controller design.

Discussion of the Linearity

In Fig. 7 the dependency of the radial force F_x on different parameters is shown for small airgaps of 250 µm. For Fig. 7(a) the rotor is assumed to be in its center position. With the magnetomotive force θ_{cx} varying and θ_{cy} set to zero ampere-turns, three curves for the force F_x for three different magnetomotive forces θ_{cz} are depicted. One can see that θ_{cz} from the axial axis has an influence on the radial force but still the relation between the current i_x and the force F_x is linear for all cases. The influence of θ_{cz} gets obvious as we look at the coupling flux $\Phi_{z\text{-}coupling}$ in Fig. 4. This flux increases the main flux created by θ_{cx} in the negative airgap x_-, but decreases the main flux in the positive airgap x_+. So the force-current relation in the x-axis is weakened for positive z-currents as shown in Fig. 7(a). The situation changes when an additional radial displacement $x = 150$ µm occurs. The relation between the force F_x and the magnetomotive force θ_{cx} becomes highly non-linear. Such a non-linear characteristic and the coupling to the other axes' parameters can pose severe problems for the control of the rotor position.

In order to characterize the force-current relation let us rewrite the aforementioned relation (2) in another way. The carrying force is determined by the magnetic fluxes Φ_{x+} and Φ_{x-} in the airgaps. These magnetic fluxes again, depend on the different magnetomotive forces and the value of the reluctances. Assuming the rotor in its center position means that the two reluctances in each axes are identical. Further we assume the control currents in the y- and z-axis to be zero. Since the two opposing reluctances in one axis are equal, the magnetic flux is split equally in the two airgaps and therefore the magnetic flux in the positive airgap is $\Phi_{x(PM)} + \Phi_{x(cx)}$ whereas the magnetic flux in the negative airgap results in $\Phi_{x(PM)} - \Phi_{x(cx)}$ as can be verified in Fig. 4. Consequently the total magnetic flux in either airgap is driven by the permanent magnet and the control coil in the x-axis and therefore the force in the x-axis can be written as:

$$F_x \propto \Phi_{x+}^2 - \Phi_{x-}^2 = (\Phi_{x(PM)} + \Phi_{x(cx)})^2 - (\Phi_{x(PM)} - \Phi_{x(cx)})^2 = 4 \cdot \Phi_{x(PM)} \Phi_{x(cx)} = k\theta_{cx}. \quad (5)$$

Again the linear relationship between the force F_x and the control current θ_{cx} can be seen. This

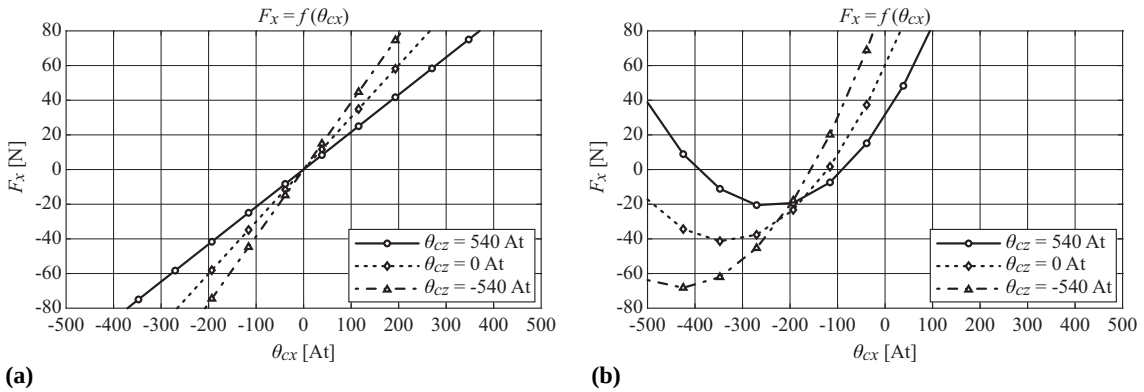

Fig. 7. Calculation of the radial force-current relation for (a) $x = 0$ µm and (b) $x = 150$ µm for a nominal airgap of $\delta = 250$ µm.

linear dependency is no longer valid if we have a displacement in the x-direction. Since the magnetic fluxes don't split equally in the airgaps the relation $F_x = f(\theta_{cx})$ will also have a quadratic as well as a constant component. The rotor is assumed to be in its axial center point, which means that $R_{z+} = R_{z-} = R_z$. If the rotor is also in its radial center position then the reluctances in the four airgaps have all the same value R. Deflecting now the rotor in x-direction will increase the airgap reluctance on one side and decrease it by the same amount on the other side such that $R_{x+} = R - \Delta R$ and $R_{x-} = R + \Delta R$. The invariant reluctances of the permanent magnet, the axial airgap, the stator, the shell and the rotor are concentrated into an equivalent reluctance R_{eq}. With these assumptions, the force-current relation for the radial force F_x can be written as:

$$F_x \propto \left\{\frac{\left[8R_{eq}^2 R\Delta R + 6R_{eq}R^2\Delta R + R^3\Delta R\right]}{\left[\tfrac{1}{2}R(R^2-\Delta R^2) + R_{eq}(2R^2-\Delta R^2)\right]^2}\right\}\theta_{cx}^2 + \left\{\frac{2\theta_{PM}\left[R_{eq}R\left(2R^2+\Delta R^2\right) + \tfrac{1}{2}R^2\left(R^2+\Delta R^2\right)\right]}{\left[\tfrac{1}{2}R(R^2-\Delta R^2) + R_{eq}(2R^2-\Delta R^2)\right]^2}\right\}\theta_{cx} + \left\{\frac{R^3\Delta R}{\left[\tfrac{1}{2}R(R^2-\Delta R^2) + R_{eq}(2R^2-\Delta R^2)\right]^2}\right\}, \quad (6)$$

which can be simplified to

$$F_x \propto A\cdot\theta_{cx}^2 + B\cdot\theta_{cx} + C. \quad (7)$$

In contrast to (5) the relation between force and current is now non-linear. Looking at formula (7) we define the linearity as

$$\text{Linearity} = \frac{B}{A\cdot\theta_{cx}}, \quad (8)$$

in order to quantify the non-linearity of the force-current relation. Since the linearity of the force-current relation can affect the stability of the position controller it must be the goal to minimize such non-linearities. Formula (8) directly shows that the linearity will deteriorate with increasing control currents. This does not pose severe problems since at steady state operation the control currents should be moderate. The effect of two other parameters which can be changed is shown in Fig. 8. In the diagram on the left side the influence of the size of the permanent magnet can be seen. A bigger permanent magnet leads to a better linearity. In Fig. 8(b) it is clearly shown that an increased airgap size has a positive effect on the linearity of the force-current relation. Here the airgap δ is the same for the radial and the axial bearing.

However, the charts in Fig. 7 show that in all situations there is an ampere-turns value θ_{cx}, for which the rotor can be pulled to and held in the center position. In such a stationary analysis the rotor can be stabilized by a correct choice of the control current. However, it is important to keep in mind that with a too narrow airgap the stabilization can be much more difficult to achieve since the controller has to guarantee a stable operation even under non-linear conditions. This is not trivial since a magnetic bearing on its own is already challenging in terms of stable control due to the inherent unstable characteristics of the control path. A proper selection of the PID controller gains is a basic requirement for a stable operation. If the control path changes such strongly as described in Fig. 7

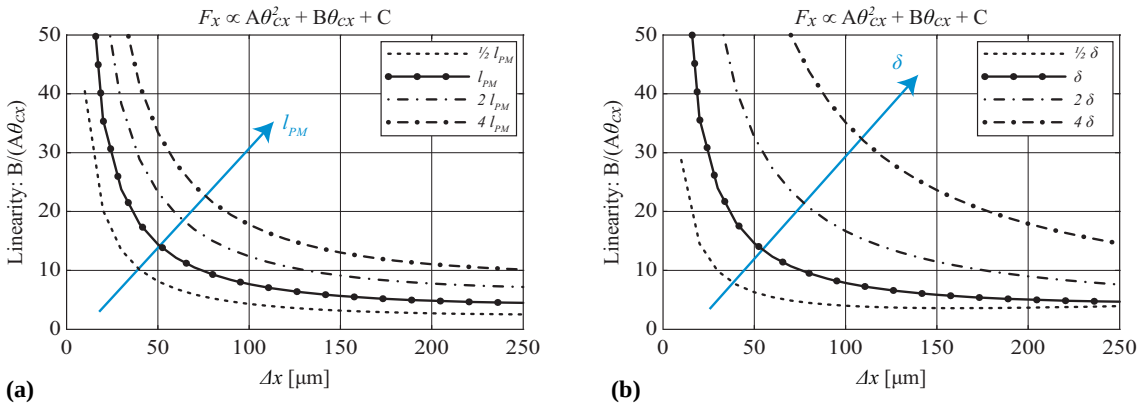

Fig. 8. Effect on the linearity of the force-current relation of (a) the permanent magnet and (b) of the airgap size.

due to different operating points of the bearing, it will be a big challenge for a stable control within the whole range of operation.

Effects on the control

The main challenge in a magnetic bearing is always a stable and robust levitation of the rotor either in its centre position or in another predefined position. The control of the rotor position will be implemented as cascaded position controller. To study the effects of the non-linear relations in the magnetic bearing system the cascaded controller was implemented as a Matlab/Simulink model. The performance of the controller was first tested by defining the force according the well-known relation (2) where k_i and k_r are taken from the simplest operating point where the rotor is in its centre position and no control currents are injected into the coils. The bearing parameters k_i and k_r are assumed to remain constant for any position the rotor can reach and for any current injected in the coils. For such a model it is possible to find a PID parameter set (K_P, T_I, T_D) which can follow a sinuiodal setpoint function. It should now be investigated if the aforementioned non-linear characteristics of the bearing forces pose a problem for such a controller. To simplify the problem only the definition of the force for the x-axis is made variable. All the other bearing parameters are left unchanged. As it can be observed in Fig. 7(b) the force F_x no longer depends linearly on the control magnetomotive force θ_{cx} if the rotor is deflected in x-direction. Knowing that the magnetomotive force θ_{cx} is directly related to the control current i_x via the number of turns, the relation of the force F_x and the control current can now described by a function according the following polynomial equation:

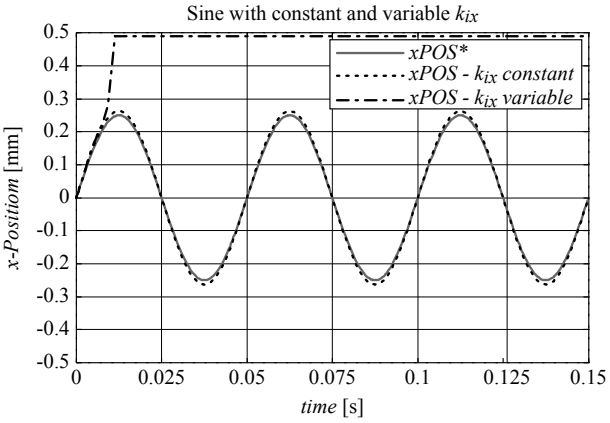

Fig. 9. Controlled x-position following a sinusoidal set-point.

$$F_x = a(x)\cdot i_x^2 + b(x)\cdot i_x + c(x), \tag{9}$$

where the polynomial coefficients were derived from calculations with the equivalent circuit model of the bearing as depicted in Fig. 4. These coefficients were then integrated in the simulation model of the controller. In reality however, the polynomial coefficients are also dependent on the rotor deflection in the other directions and also depend on the control currents in the other coils. This fact has been omitted in order to simplify the problem. In Fig. 9 the rotor position should follow a sinusoidal setpoint function. If we implement the constant bearing parameters for all rotor positions, then there can be found a PID parameter set (K_P, T_I, T_D) which makes the rotor follow the setpoint function. Now it should be checked if the controller works as well if the force F_x is dependent on the rotor position according to (9). As can be seen in Fig. 9 this is not the case for the same set of PID parameters. The x-position of the rotor cannot follow the sinusoidal setpoint function and the rotor can't be pulled to the centre anymore with this set of PID parameters.

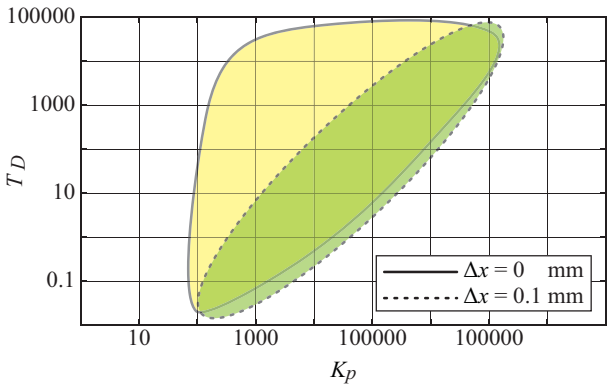

Fig. 10. Stable parameter sets (K_P, T_D) for two different operating points.

Thus, it is essential to implement the correct definitions for the different forces with their dependencies on the current operating point of the magnetic bearing in order to optimize the position controller. It can then be analyzed what set of parameters can stabilize the rotor for different operating points. The set of possible parameters

(K_P, T_D; whereas T_I=0) for two different operating points were analyzed and are depicted in Fig. 10. It can be seen that in this case the two stable areas overlap. Nevertheless it is important to identify the stable parameter sets for different operating points, such that the controller can be fed with either a parameter set which is stable over the whole operating range or a parameter set which is appropriate for the current operating point.

Summary

For high-speed machines the use of conventional ball bearings brings some drawbacks as high losses and limited lifetime. An active magnetic bearing is an alternative bearing topology, which is suitable for high-speed operation. Due to the compact size of the electrical machine at these high-speeds, it is important to minimize the volume of the magnetic bearing as well. In this paper, an active magnetic bearing that has the radial and axial forces combined into a single bearing unit was presented.

One of the critical and challenging research topics for active magnetic bearings is the analysis of the magnetic forces, their dependencies and their couplings. For this purpose, a simple analytical model of the bearing was described. With this model the bearing forces were discussed and some important dependencies and couplings were pointed out. Furthermore different ways to minimize the non-linearity of the force-current relation have been presented. To validate the analytical model it has been compared to the results of 3D-FEM simulations of the chosen bearing system. The simulation results showed a good accordance with the analytical results, which confirms the proposed model. Both approaches clearly showed the nonlinear characterization of the bearing forces depending on the bearing's current operating point. It can be concluded that the correct description of the bearing forces is crucial in order to design the position controller. It may be even necessary to adapt the controller gains during operation according the current operating point. Further research in that field will be focused on the analysis of small-signal and large-signal stability of the control for such a coupled system under consideration of decoupling networks. Furthermore, the cross-coupling between the bearing axes shall be minimized and geometrical parameters will be studied in order to achieve stable control behavior.

References

[1] C. Zwyssig, M. Dürr, S.D. Round and J.W. Kolar, "An Ultra-High-Speed, 500'000 rpm, 1 kW Electrical Drive System," 4th Power Conversion Conference 2007, Nagoya, Japan, April 2-5, 2007.

[2] M. A. Rahman, A. Chiba, and T. Fukao, "Super high speed electrical machines – summary," IEEE Power Engineering Society General Meeting, June 6-10, 2004, vol. 2, pp. 1272 – 1275.

[3] J. Oyama, T. Higuchi, T. Abe, K. Shigematm X. Yang, E. Matsuo, "A trial production of small size ultra-high speed drive system," IEMDC2003, vol. 1, no.2-1-1, pp. 31 – 36, 2003.

[4] MiTi Developments (November 2005). "Oil-free, motorized, automotive fuel cell air compressor/expander system," Available: http://www.miti.cc

[5] B. H. Bae, S. K. Sul, J. H. Kwon, and J. S. Byeon, "Implementation of sensorless vector control for super-highspeed PMSM of turbo-compressor," IEEE Trans. on Industry Applications, vol. 39, no. 3, pp. 811 – 818, May-Jun. 2003.

[6] S. A. Jacobson and A. H. Epstein, "An informal survey of power MEMS," ISMME2003, Tsuchiura, Japan, December 1 – 3, 2003,pp. 513 – 520.

[7] P.T. McMullen, S. Huynh, „Magnetic Bearing Providing Radial and Axial Load Support for a Shaft," U.S. Patent 5,514,924, May 7, 1996.

[8] Maxwell 3D by Ansoft Corporation [Online].
Available: http://www.ansoft.com.